

EXPERIMENTAL STUDIES ON SECONDARY ELECTRON EMISSION CHARACTERISTICS FOR CHAMBER MATERIALS OF ACCELERATORS*

Y. Liu[†], W. Liu, Y. Jiao, Z. Duan, Institute of High Energy Physics (IHEP),
Chinese Academy of Sciences (CAS), Beijing 100049, China,
S. Liu, P. Wang, Dongguan Institute of Neutron Science (DINS), Dongguan 523803, China

Abstract

Secondary electron emission (SEE) of surface is the origin of multipacting effect which could seriously deteriorate beam quality and even perturb the normal operation of particle accelerators. Experimental measurements on secondary electron yield (SEY) on different materials and coating have been developed in many accelerator laboratory. In fact, the SEY is just one parameter of secondary electron emission characteristics which include spatial and energy distribution of emitted electrons. A novel experimental apparatus was set up in China Spallation Neutron Source (CSNS) and innovative measurement methods were applied to obtain the whole characteristics of SEE. With some traditional accelerator chamber materials such as Cu, Al, TiN, et al., SEY dependence on primary electron energy and beam injection angle, spatial and energy distribution of emitted secondary electrons were achieved with this measurement apparatus.

INTRODUCTION

The secondary electron emission (SEE) and accumulation is one of the critical limits on the performance of high current accelerator, such as vacuum deterioration, beam instability, beam losses, emittance growth, beam lifetime decline, and additional heat loads for a cryogenic vacuum chamber [1-3]. The experimental investigation on SEE has attracted so many interests over the past decades. Many accelerator laboratories, such as SLAC, KEK, FERMI LAB, and CERN have set up an experimental apparatus to measure secondary electron yield (SEY) for different materials with or without coating [4-6]. However, the SEY is just one parameter of secondary electron emission characteristics which also include spatial distribution and energy spectrum of emitted electrons. The spatial distribution and energy distribution were ignored in most experimental measurements. In order to understand the whole information on SEE, a new type of experimental platform was set up in China Spallation Neutron Source (CSNS). In this paper the experimental methods by a movable sample holder and RFA (Retarding Field Analyser) to obtain electron spatial distribution and energy spectrum of secondary electrons are introduced. Then, with some different materials sampled adopted in accelerators, the detailed characteristic parameters are measured with this experimental apparatus.

* Work supported by Foundation of Key Laboratory of Particle Acceleration Physics and Technology, IHEP, CAS (JSQ2016ZZ02); National Natural Science Foundation of China (11275221, 11375215);
[†] email address: liuyd@ihep.ac.cn.

MEASUREMENT METHODS AND EXPERIMENTAL APPARATUS

The measurement principle on SEE is explained in Figs. 1(a)–1(c). The movable sample holder is wrapped by a retarding field analyser. The RFA is composed of a cap detector (connected with terminal A) and a cylindrical wall detector (connected with terminal B) with meshed grid (connected with terminal C) and ground electrodes (connected with terminal E) inside. There is an insulating ring between the cap detector and wall detector for spatial distribution measurement shown in Fig. 1(b). In order to get the secondary electron emission coefficient more accurately, the sample (connected with terminal D) is connected with a DC bias source. The ground electrode is used to shield the electrostatic field and reduce its impact on the electron beam. When the bias voltage is -20 V, the secondary electrons are allowed to escape the surface of the sample fully and the sample current I_s is measured. By regulating the bias voltage to +100 V which is high enough to prevent secondary electrons from escaping from the sample, the primary electron current I_p is obtained, as shown in Fig. 1(a). With correction on the energy of primary beam from bias voltage -20 V, the energy calibration is included in the experiments. With measured I_s and I_p , the secondary electron emission coefficient is recorded as $\delta = I_s/I_p = 1 - I/I_p$. For the sake of SEY dependence on the incident angle, the sample holder can be rotated from 0° to 90° , shown in Fig. 1(a).

For spatial distribution measurement, the picoammeter was connected with terminal B. The experimental principle is to move the sample holder to different vertical positions and measure current variations on the cylindrical wall detector, as shown in Fig. 1(b). Assuming the sample's initial vertical position is M and the half flare angle of the sample is α as shown in Fig. 1(b), the measured current on cylindrical wall detector is I_α ; after slightly moving the sample to another position N , the measured current on the wall collector is $I_{\alpha+\Delta\alpha}$ and the angle and current variation are $\Delta\alpha$ and $\Delta I_\alpha = I_\alpha - I_{\alpha+\Delta\alpha}$, respectively. Varying the sample position step by step, the azimuthal distribution is achieved. Using cylindrical wall detector for obtaining the secondary electron (SE) current ΔI_α can avoid the measured electrons leaking from the aperture on the top of the cap detector.

The RFA which is the capped cylindrical wall detector with two meshed grid layers inside is used for scanning the secondary electron energy spectrum. By scanning the

Content from this work may be used under the terms of the CC BY 3.0 licence (© 2018). Any distribution of this work must maintain attribution to the author(s), title of the work, publisher, and DOI.

voltage on the grid layer with a DC voltage source, the energy spectrum can be obtained, as shown in Fig. 1(c).

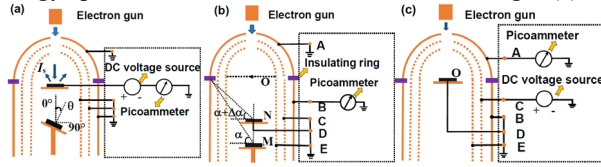


Figure 1: Schematic diagram on the measurement of secondary electrons' characteristics.

The SEE experimental platform is composed of a vacuum system, electron gun, removable sample holder, and RFA for measuring secondary electrons. The vacuum system can keep the sample in a high vacuum environment with pressure about 10^{-6} Pa. The Kimball Physics EGL-7 electron gun was installed and directed toward the sample vertically, and the electron beam energy ranges from 100 eV to 5 keV with the emission current span from 1 nA to 100 μ A. The maximum movable vertical distance of the sample holder is about 150mm which corresponds to the spatial angle 10° – 80° . The photograph and partial view of the apparatus are shown in Fig. 2.

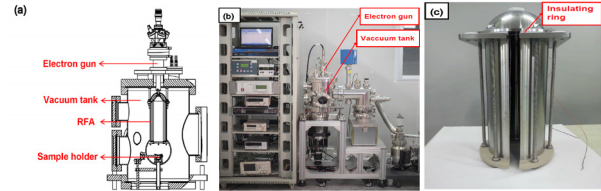


Figure 2: The partial view and photograph of the apparatus and RFA: (a) partial view of experimental setup, (b) schematic of the experimental setup, (c) structure of RFA.

EXPERIMENTAL RESULTS

The characteristic parameters determining the secondary electron emission are SEY, the secondary electron energy spectrum and its spatial distribution. With this apparatus and methods described in section II, the samples, Cu, Al, Stainless Steel, TiN, TiZrV and Si, were measured.

SEY and its Dependence on Incidence Angle

The SEY measurements were carried out with the electron beam at normal incidence from 60 eV to 1480 eV with current of hundreds of nA. The SEY results as a function of the primary energy are shown in Fig. 3(a, b).

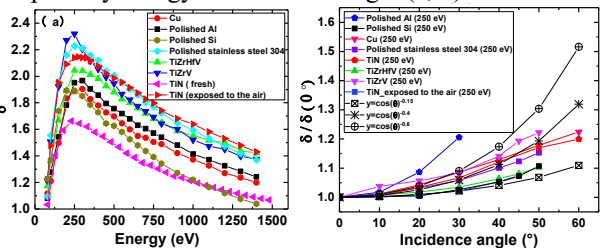


Figure 3: SEY on different samples and its dependence on incident angle (a: $\theta=0^{\circ}$; b: SEY with different θ).

It is clear that the SEY for TiN coating with the lowest yield may be the best choice for beam chamber. The SEY

increases with the injection angle and its relation can be fitted by cosine function, $\delta=(\cos\theta)^n$. The fitted parameter n for different materials are summarized in Table 1.

Table 1: The Fitted Parameters n for Different Samples

sample	n
Cu	0.25~0.5
TiN	0.15~0.4
TiZrHfV	0.15~0.4
TiZrV	0.4~0.8

Spatial Distribution of SEE

The sample holder is pushed vertically by an actuator step by step to change the spatial azimuth of the secondary electrons distributed. During the movement, the primary beam energy and emission current is fixed at 600 eV and 1.5 μ A, respectively. The ratio between secondary electron current I_s , and primary electron current I_p in different azimuth was used to explore the azimuthal distribution. The measured transparency on meshed grid electrode and ground electrode was stable at 63% during the movement of sample holder. The measured SE spatial distribution is shown in Fig. 4.

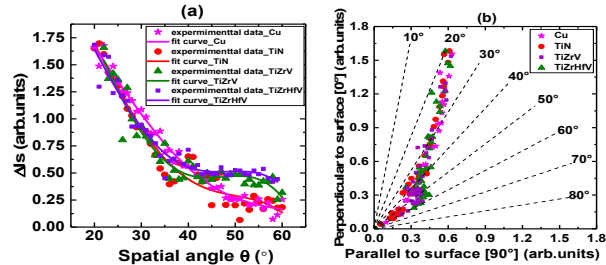


Figure 4: Spatial distribution of secondary emission electrons.

((a): in Cartesian, (b): in Polar coordinate systems)

The SEY of the unit solid angle is proportional to the following formula [7]:

$$f(\theta) = \cos\theta(1 + a \sin^2\theta + b \sin^4\theta + \dots) \quad (1)$$

where a , b are the coefficients that change with smallest momentum that electrons need to escape the sample slowly. The fitted parameters, a and b are summarized in Table 2. It is clear that the spatial distribution of secondary electrons from different materials is almost the same.

Table 2: The Fitted Parameters of Spatial Distribution

samples	a	b
Cu	-2.10265	1.632612
TiN	-1.23562	1.914979
TiZrHfV	-1.0863	2.026681
TiZrV	-0.95964	1.989641

Spectrum Distribution of SEE

Fixing the injection electron beam energy E_p at 150 eV, 200 eV, 250 eV, and the collected secondary electron energy spectrum is measured by RFA, and the results are shown in Fig. 5. According to the normal secondary electron emission model [8], the secondary electrons are composed of three sources: “true” secondary electrons with the lower energy range, 0~50 eV; “elastic” electrons

which are emitted with almost the same energy as incident particles; and “rediffused” electrons with uniform energy spectrum from 50 eV to the incident particle energy. For this experiment on samples, the “true” secondary electrons energy ranged from 0 to 50 eV with peak at about 5 eV which doesn’t change with the energy of incident electrons.

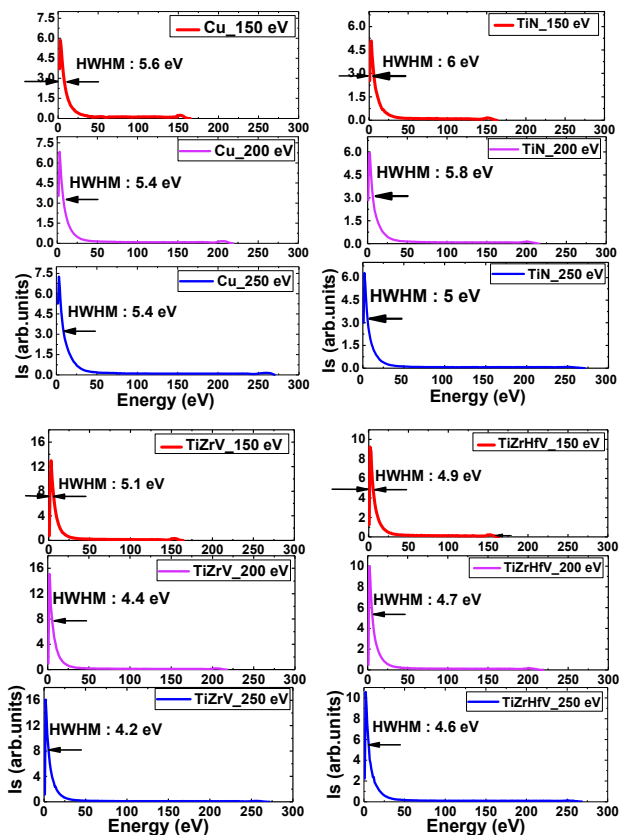


Figure 5: Spectrum distribution of SEE.

Accordinging Fig. 5, the first peak means the “true” secondary electrons, and the energy of “elastic” electrons will change with the different incident electron energy. The percentage for “elastic” is more than 80% of the total emission electrons. The percentage for “true”, “elastic” and “rediffused” secondary electrons is listed in Table 3.

Table 3: The Percentage for Various Secondary Electrons

Samples	E_p (eV)	SE	ERE	IRE
Cu	150	80.2%	4.8%	15.0%
	200	79.9%	3.1%	17.0%
	250	76.8%	2.9%	20.3%
TiN	150	81.8%	3.3%	14.9%
	200	78.7%	3.5%	17.8%
	250	78.5%	3.0%	18.5%
TiZrHfV	150	83.5%	3.1%	1.4%
	200	80.7%	2.7%	16.6%
	250	78.5%	2.4%	19.1%
TiZrV	150	84.8%	2.8%	12.4%
	200	84.2%	2.2%	13.6%
	250	83.3%	1.8%	14.9%

SEY Depression as Electron Dose Deposition

The incident electron bombardment can cause surface changes of the material, such as clearance of some contaminants and oxide [9]. After longer bombard by primary electrons with proper energy, the surface graphitization may be produced and the presence of the carbon film depresses the secondary electron yield to a lower level. In order to understand the “dose” effect, the SEY is measured in different deposition of primary beam, shown in Fig. 6. Fixing the primary beam energy and current at 250 eV and 0.61 μA with continuous bombardment on the sample for 10 hours corresponding the charge deposition of $2.46 \times 10^{-3} \text{ C/mm}^2$, the maximum SEY drops from 1.81 to 1.46.

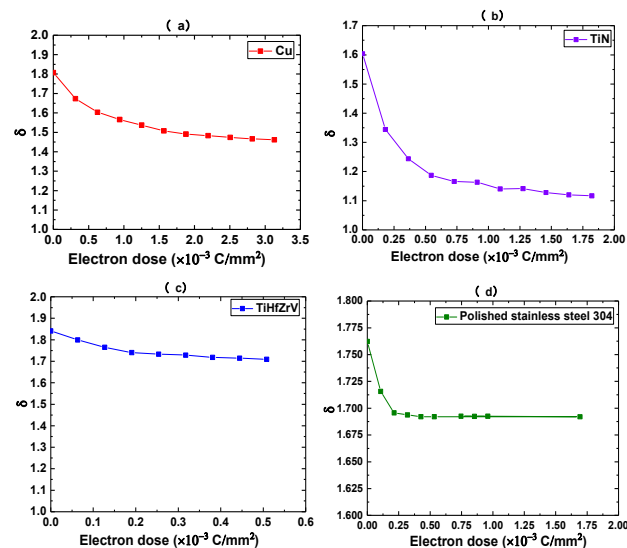


Figure 6: SEY as a function of electron dose.

CONCLUSION

A novel experimental apparatus for SEE measurements was set up in CSNS. The SEE characteristics including SEY, spatial distribution, energy spectrum, and “dose” effect, were obtained by this device. The measurement results proved the SEY dependence on spatial angle and SE spatial distribution can be applied with cosine relation. The “true” secondary electron energy range (<50 eV) for different materials have been verified in energy distribution measurements. The experimental results testified the availability on measurement methods and the apparatus structure.

REFERENCES

- [1] R. Cimino and T. Demma, “Electron cloud in accelerators”, *Int. Journal of Modern Phys. A*, vol. 29, no. 17, p. 1430023, 2014.
- [2] J. A. Crittenden *et al.*, “Investigation into electron cloud effects in the International Linear Collider positron damping ring”, *Physical Review Special Topics-Accelerators and Beams*, vol. 17, no. 3, p. 031002, 2014.
- [3] R. Prakash, A. R. Jana and V. Kumar, “Multipacting studies in elliptic SRF cavities”, *NIM A*, vol. 867, pp. 128-138, 2017.
- [4] R. Cimino *et al.*, “Detailed investigation of the low energy

secondary electron yield of technical Cu and its relevance for the LHC”, *Physical Review Special Topics-Accelerators and Beams*, vol. 18, no. 5, p. 051002, 2015

- [5] K. Yamamoto *et al.*, “Secondary electron emission yields from the J-PARC RCS vacuum components”, *Vacuum*, vol. 81, no. 6, pp 788-792, 2007.
- [6] Y. Ji, L. Spentzouris and, R. Zwaska, “Update of the SEY Measurement at Fermilab Main Injector”, in *Proc. NAPAC’16*, Chicago, IL, USA, Oct. 2016.
doi:10.18429/JACOW-NAPAC2016-THPOA45
- [7] J. Jonker, “The angular distribution of the secondary electrons of nickel”, *Philips Research Reports*, vol. 6, no. 5, pp. 372-387, 1951.
- [8] H. Seiler, “Secondary electron emission in the scanning electron microscope”, *Journal of Applied Physics*, 1983, vol. 54, no.11, pp. R1-R18.
- [9] R. Cimino *et al.*, “Electron energy dependence of scrubbing efficiency to mitigate e-cloud formation in accelerators”, in *Proc. EPAC08*, Genoa, Italy, 23-27 June 2008, paper TUPP027, pp.1592–1594.